Physics Letters A 580 (2026) 131488

Contents lists available at ScienceDirect

Physics Letters A

journal homepage: www.elsevier.com/locate/pla

Letter

Quantum phase transitions on complex projective space $\mathbb{CP}^2$

Xue Meng [a,b], Junwen Zhao [b], Wei Zhu [b,c,*], Congjun Wu [b,c]

[a] Department of Physics, Fudan University, Shanghai, 200433, China
[b] Department of Physics, School of Science, Westlake University, Hangzhou, 310030, China
[c] Institute of Natural Sciences, Westlake Institute for Advanced Study, Hangzhou, 310024, China

ARTICLE INFO

Editor: Lilia Woods

PACS:
73.43.Cd
03.65.Ud
05.30.Pr

Keywords:
Quantum phase transition
Landau level projection
Higher dimension

ABSTRACT

Traditional microscopic studies of phase transitions are mostly performed on the discretized lattices living in the spatial dimensions less than three, whereas higher-dimensional cases have been much less explored. Here we explore the realization of one quantum phase transition on the four-dimensional complex projective space $\mathbb{CP}^2$ geometry. We propose a computationally efficient phenomenological modeling framework based on Landau level regularization. As a first demonstration, we construct a microscopic model that realizes a spontaneous symmetry-breaking phase transition belonging to the $(4+1)$D Ising universality class. Our numerical results confirm that the finite-size scaling of the order parameter is consistent with the Landau theory expectation. The present approach can be generalized to study various other universality classes, opening a route toward systematic investigations of phase transitions on higher-dimensional manifolds.

1. Introduction

While our physical world is three-dimensional, many interesting and important mathematical theories are defined in higher dimensions. Studying such higher-dimensional theories is not merely a formal generalization, instead it helps to chart the intrinsic landscape of the theory itself, uncover universal principles, identify its limitations, and forging indispensable connections to broader structures in theoretical physics and pure mathematics. Famous examples include the supersymmetric Yang-Mills theory in the spacetime dimension equal to four [1] and five [2,3], as representative examples.

Traditionally, these higher-dimensional theories are extremely challenging to study in a non-perturbative and microscopic way, primarily due to the limited computational resources available. Consider conventional lattice simulations: the Hilbert space dimension typically grows exponentially with the system size L. As a concrete example, for the $(4+1)$-D transverse Ising model, exact diagonalization is essentially restricted to $L=2$ (corresponding to the number of lattice sites $N=L^4=16$), equivalent to only two lattice sites in each spatial direction. For $L=3$, where $N=L^4=81$, the problem becomes completely out of reach. This is the main reason that, it is still lacking of a microscopic simulation of quantum models on $(4+1)$-D or higher dimensions, to our best knowledge. In this sense, straightforward lattice simulations in higher dimensions are not practical, and it is therefore desirable to develop some alternative approaches for modeling quantum systems in higher-dimensional spaces.

Very recently, it has been proposed to study the critical field theories on the fuzzy two-sphere geometry (here the two-sphere S^2 is equivalent to the complex projective space $\mathbb{CP}^1$ manifold). So far various critical field theories have been studied, including Ising and $O(N)$ Wilson-Fisher universality classes [4–7], Lee-Yang universality class [8–10], Potts model [11], free boson theory [12,13], deconfined quantum criticality [14–17], QED-Chern-Simons theory [18], surface criticality and defect criticality [19–22], just to name a few. The key idea involved here is based on the Landau level quantization scheme on the two-sphere or $\mathbb{CP}^1$ manifold [23].In addition, Landau quantization can also be formulated on the four-dimensional S^4 geometry as shown by Hu and Zhang [24], on the complex projective space $\mathbb{CP}^2$ by D. Karabali and V.P. Nair, and more generally on $\mathbb{CP}^k$ in arbitrary even dimensions [25,26]. It is therefore natural to ask whether a similar Landau level projection strategy can be employed to investigate critical theories in higher-dimensional spacetime.

In this work, mainly motivated by the recent progress on the simulation of quantum phase transitions on the two-sphere geometry (equivalent to the complex projective space $\mathbb{CP}^1$ manifold) via the projected Hamiltonian method, we explore the realization of quantum critical theory on the $\mathbb{CP}^2$ geometry which is $(4+1)$-D. Our key step is to utilize the Landau level projection which greatly truncates the Hilbert space but

* Corresponding author.
E-mail address: zhuwei@westlake.edu.cn (W. Zhu).

https://doi.org/10.1016/j.physleta.2026.131488
Received 24 November 2025; Received in revised form 4 February 2026; Accepted 16 February 2026
Available online 25 February 2026
0375-9601/© 2026 Elsevier B.V. All rights are reserved, including those for text and data mining, AI training, and similar technologies.

keeps all the symmetries of the geometric $\mathbb{CP}^2$ space. As a first example, we construct a (4+1)-D quantum Ising transition on a $\mathbb{CP}^2$ manifold. We use exact diagonalization(ED) and density-matrix renormalization group(DMRG) to simulate different system sizes with up to 28 effective spins. By using finite-size scaling method we verify the Landau-Ginzburg theory. Our results offer a new path for simulation of phase transitions in higher space-time dimensions.

This paper is organized as follows. In Section 2.1, we review the background knowledge including the quantized Landau level and corresponding single particle wavefunction on $\mathbb{CP}^2$ space in the presence of $U(1)$ magnetic field. In Section 2.2, we discuss the case of spinless many-body fermion systems with fractional filling and two-body interactions which are formulated on $\mathbb{CP}^2$ Landau levels. In Section 3.1, we propose a model to realize the (4+1)-D Ising transition on $\mathbb{CP}^2$ space. In Section 3.2, we describe the numerical methods employed. In Section 3.3, we apply the finite-size scaling analysis to determine the corresponding critical point and critical exponents. At last, summary and discussion are provided in Section 4.

2. Review of background

In the QHE, the energies of electrons moving under a magnetic field are quantized into discrete values known as Landau levels. Haldane [23], together with the earlier foundational work by Wu and Yang [27,28], constructed Landau levels on a spherical manifold(S^2 is equivalent to $\mathbb{CP}^1$) with a $U(1)$ monopole and applied it to the fractional quantum Hall problem. In this section, we focus on the lowest Landau level(LLL) states on the 4-dimensional geometry $\mathbb{CP}^2$ with $U(1)$ monopole following the discussions in Ref [25,26,29–31], which can be generalized on $\mathbb{CP}^k$ spaces. In this paper, the general results for $\mathbb{CP}^k$ geometry are summarized in Appendix A, and the main text focuses on the $\mathbb{CP}^2$ case in greater detail. In the following, we take $\hbar = c = e = 1$.

2.1. $\mathbb{CP}^2$ Landau levels and the lowest Landau level projection

The complex projective space $\mathbb{CP}^2$ is a 4-dimensional manifold that can be expressed as the coset space

$$\mathbb{CP}^2 = \frac{SU(3)}{SU(2)\times U(1)}, \tag{1}$$

This geometric structure naturally supports background gauge fields with $U(1)$ or $SU(2)$ symmetry.

The symmetry group of CP^2 is $SU(3)$ which has 8 generators [32]:

$$\hat{\lambda}_1 = \begin{pmatrix} 0 & 1 & 0 \\ 1 & 0 & 0 \\ 0 & 0 & 0 \end{pmatrix}, \quad \hat{\lambda}_2 = \begin{pmatrix} 0 & -i & 0 \\ i & 0 & 0 \\ 0 & 0 & 0 \end{pmatrix}, \quad \hat{\lambda}_3 = \begin{pmatrix} 1 & 0 & 0 \\ 0 & -1 & 0 \\ 0 & 0 & 0 \end{pmatrix},$$
$$\hat{\lambda}_4 = \begin{pmatrix} 0 & 0 & 1 \\ 0 & 0 & 0 \\ 1 & 0 & 0 \end{pmatrix}, \quad \hat{\lambda}_5 = \begin{pmatrix} 0 & 0 & -i \\ 0 & 0 & 0 \\ i & 0 & 0 \end{pmatrix}, \quad \hat{\lambda}_6 = \begin{pmatrix} 0 & 0 & 0 \\ 0 & 0 & 1 \\ 0 & 1 & 0 \end{pmatrix}, \tag{2}$$
$$\hat{\lambda}_7 = \begin{pmatrix} 0 & 0 & 0 \\ 0 & 0 & -i \\ 0 & i & 0 \end{pmatrix}, \quad \hat{\lambda}_8 = \frac{1}{\sqrt{3}}\begin{pmatrix} 1 & 0 & 0 \\ 0 & 1 & 0 \\ 0 & 0 & -2 \end{pmatrix}.$$

It is clear that $\{\lambda_1, \lambda_2, \lambda_3\}$ generate the $SU(2)$ subalgebra, and λ_8 generate the $U(1)$ subalgebra.

It is useful to redefine the generators as $\hat{F}_i = \frac{1}{2}\hat{\lambda}_i$ which is consistent with the definition we used before in Eq. (A.3) so that the Lie algebra is:

$$[\hat{F}_i, \hat{F}_j] = i f_{ijk}\hat{F}_k, \tag{3}$$

with anti-symmetric structure constant $f_{ijk} = -f_{jik}$. We can now define the ladder operators as follows:

$$\hat{T}_\pm = \hat{F}_1 \pm i\hat{F}_2, \qquad \hat{V}_\pm = \hat{F}_4 \pm i\hat{F}_5, \qquad \hat{U}_\pm = \hat{F}_6 \pm i\hat{F}_7,$$
$$\hat{T}_3 = \hat{F}_3, \qquad \hat{Y} = \frac{2}{\sqrt{3}}\hat{F}_8. \tag{4}$$

One can see that in this definition, the right actions of $\{\hat{T}_\pm, \hat{T}_3\}$ and $\hat{F}_8$ are indeed the $\hat{R}_\alpha$ and $\hat{R}_{k^2+2k}$ respectively in $\mathbb{CP}^k$ case, corresponding to the $SU(k)$ and $U(1)$ background charge. And the right actions of remaining operators $\{\hat{U}_\pm, \hat{V}_\pm\}$ correspond to the raising and lowering operators $\hat{R}_{\pm i}, i = 1, 2$ that are in the implement of $U(k)$.

By using of the structure constant, for example $f_{458} = f_{678} = \frac{\sqrt{3}}{2}, f_{345} = -f_{367} = \frac{1}{2}, \ldots$, the commutation relations for these operators can be derived:

$$[\hat{T}_3, \hat{T}_\pm] = \pm\hat{T}_\pm, \quad [\hat{T}_+, \hat{T}_-] = 2\hat{T}_3,$$
$$[\hat{T}_3, \hat{U}_\pm] = \mp\frac{1}{2}\hat{U}_\pm, \quad [\hat{U}_+, \hat{U}_-] = \frac{3}{2}\hat{Y} - \hat{T}_3 \doteq 2\hat{U}_3,$$
$$[\hat{T}_3, \hat{V}_\pm] = \pm\frac{1}{2}\hat{V}_\pm, \quad [\hat{V}_+, \hat{V}_-] = \frac{3}{2}\hat{Y} + \hat{T}_3 \doteq 2\hat{V}_3,$$
$$[\hat{T}_+, \hat{V}_+] = [\hat{T}_+, \hat{U}_-] = [\hat{U}_+, \hat{V}_+] = 0,$$
$$[\hat{T}_+, \hat{V}_-] = -\hat{U}_-, \quad [\hat{T}_+, \hat{U}_+] = \hat{V}_+, \quad [\hat{U}_+, \hat{V}_-] = \hat{T}_-,$$
$$[\hat{Y}, \hat{T}_\pm] = 0, \quad [\hat{Y}, \hat{T}_3] = 0,$$
$$[\hat{Y}, \hat{U}_\pm] = \pm\hat{U}_\pm, \quad [\hat{Y}, \hat{V}_\pm] = \pm\hat{V}_\pm. \tag{5}$$

Notice that the commutator $[\hat{U}_+, \hat{U}_-]$ and $[\hat{V}_+, \hat{V}_-]$ above actually fit the results in Eq. (A.7). The operators $\{\hat{T}_+, \hat{T}_-, \hat{T}_3\}$, $\{\hat{U}_+, \hat{U}_-, \hat{U}_3\}, \{\hat{V}_+, \hat{V}_-, \hat{V}_3\}$ form a closed subalgebra $SU(2)$. This shows that all three of them are subalgebra of $SU(3)$ and each individually, which we call T-spin, U-spin or V-spin, aligns with the algebra of the angular momentum operators, represented by the Lie algebra $SU(2)$.

Since the maximum number of commuting generators of $SU(3)$ Lie algebra is 2, the rank of $SU(3)$ group is 2. We consider the commutation $[\hat{Y}, \hat{T}_3] = 0$ which means $\hat{Y}$ and $\hat{T}_3$ can be simultaneously diagonalized. Thus we can define the common eigenstates $|t_3, y\rangle$ with: $\hat{T}_3|t_3, y\rangle = t_3|t_3, y\rangle, \hat{Y}|t_3, y\rangle = y|t_3, y\rangle$. The physical interpretation of the quantum numbers of $SU(3)$ is viewing y as hypercharge and t_3 as isospin.

By using the commutation relations Eq. (5), one can easily get $\hat{T}_3(\hat{V}_\pm|t_3, y\rangle) = (t_3 \pm \frac{1}{2})(\hat{V}_\pm|t_3, y\rangle), \hat{T}_3(\hat{U}_\pm|t_3, y\rangle) = (t_3 \mp \frac{1}{2})(\hat{U}_\pm|t_3, y\rangle)$ and $\hat{Y}(\hat{V}_\pm|t_3, y\rangle) = (y \pm 1)(\hat{V}_\pm|t_3, y\rangle), \hat{Y}(\hat{U}_\pm|t_3, y\rangle) = (y \pm 1)(\hat{U}_\pm|t_3, y\rangle)$. Thus, both $\hat{V}_\pm$ and $\hat{U}_\pm$ raise the lower, respectively, the quantum number t_3 by $\frac{1}{2}$ and the quantum number y by 1. In addition, because of the relations $[\hat{Y}, \hat{T}_\pm] = 0$, the operators $\hat{T}_\pm$ do not change the quantum number y, while they only change the quantum number t_3 by integer units. The value of the isospin t_3 may be integer or half-integer because of the algebra of angular momentum, while for the value of hypercharge y, since $\hat{Y} = \frac{2}{3}(\hat{U}_3 + \hat{V}_3)$, with U_3, V_3 an integer or half-integer, the eigenvalue for $\hat{Y}$ is an integer multiple $\frac{1}{3}$, that is, $y = 0, \pm\frac{1}{3}, \pm\frac{2}{3}, \ldots$.

Therefore, we can draw the actions of these shift operators in the $t_3 - y$ plane. It is illustrated in Fig. (1a). The units of y correspond to $\frac{\sqrt{3}}{2}$ times the units on t_3 axis.

In summary, $SU(3)$ multiplets can be constructed by means of coupled $T-, U-, V-$ multiplets, and the algebra of each of them is isomorphic to $SU(2)$ algebra. And how these shift operators $\hat{T}_\pm$, $\hat{V}_\pm$, $\hat{U}_\pm$ act on the states of a $SU(3)$ multiplet is according to Fig. (1a).

There are some important properties of the structure of SU(3) multiplet. Since the states of a T-multiplets are placed along the t_3-axis and are counted by the quantum numbers t_3 with all t_3 values of a given multiplet have to be within the interval $-t_{3max} \le t_3 \le t_{3max}$ according to $SU(2)$ algebra, the $SU(3)$ multiplet has to be symmetric with respect to the y-axis. Furthermore, due to the equivalence of the three subalgebras T, U, V, the figure representing an $SU(3)$ multiplet also has to be symmetric with respect to the axis $U_3 = 0 = \frac{3}{2}y - t_3$ and $V_3 = 0 = \frac{3}{2}y + t_3$. These three symmetric axes intersect, with each pair forming the angle of 120°. Thus, the representations of $SU(3)$ multiplets within the $y - t_3$ plane have to be regular hexagons or triangles. In particular, the origin $(y = 0, t_3 = 0)$ is the center of each $SU(3)$ multiplet. This is shown in Fig. (1b).

In general, a $SU(3)$ irreducible representation can be labeled by two integers (p, q), which fix the shape and highest weight states of this representation. Consider first the state which carries the maximal weight

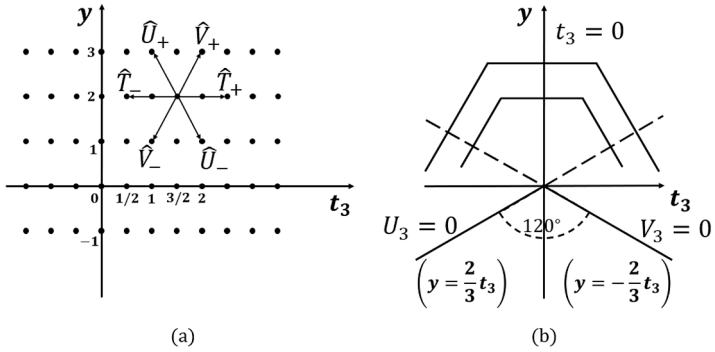

Fig. 1. (a): Action of the shift operators in $t_3 - y$ plane. (b): Symmetry of a $SU(3)$ multiplet.

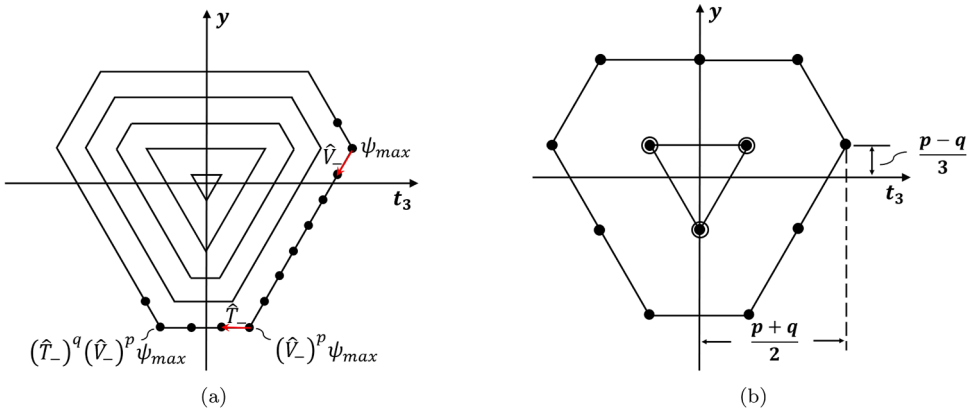

Fig. 2. (a) (p, q) representation of $SU(3)$. (b) Highest weight state with coordinates $(t_3 = \frac{p+q}{2}, y = \frac{p-q}{3})$.

t_3, which is also the rightmost state in a $t_3 - y$ figure. We denote it by $\psi_{\max} = |(t_3)_{\max}, y\rangle$. This state holds the relation:

$$\hat{T}_+\psi_{max} = \hat{V}_+\psi_{max} = \hat{U}_-\psi_{max} = 0. \tag{6}$$

Then the boundary of the multiplet can then be constructed by repeatedly applying $\hat{V}_-$ to $\psi_{\max}$ p times, followed by q times of applications of $\hat{T}_-$ to the resulting state:

$$\begin{aligned}(\hat{V}_-)^{p+1}\psi_{max} &= 0,\\ (\hat{T}_-)^{q+1}(\hat{V}_-)^p\psi_{max} &= 0,\end{aligned} \tag{7}$$

these uniquely define the integer number p, q. Thus, the numbers p and q define a multiplet of the group SU(3), describing the side length of the hexagon. It is depicted in Fig. (2). Further, this property also determines the coordinates of maximum t_3 weight state $\psi_{\max}$ in $t_3 - y$ plane: $(t_3 = \frac{p+q}{2}, y = \frac{p-q}{3})$.

It can be proved that states on the boundary of a $SU(3)$ multiplet are occupied only once. This means that there is only one state corresponding to a given point on the boundary. In the next layer, each point is occupied by two states of the multiplet. The multiplicity is increased by one each time we pass to the next inner shell until reaching q steps, the hexagon has become a triangle. Then the multiplicity will not change. Each state within the triangle has a multiplicity of $(q + 1)$. In particular, the multiplets $(S, 0)$ are the only ones consist of only nondegenerate states. Some simple multiplets of $SU(3)$ are shown as follows in Fig. (3).

By calculating the number of points in each hexagon shells and the interior points within the triangle, one can derive the dimension of the general representation $D(p, q)$[1]:

$$d(p, q) = \frac{1}{2}(p + 1)(q + 1)(p + q + 2) \tag{8}$$

[1] For $SU(3)$, the irrep (p, q) denotes the Dynkin labels $[p, q]$, and the corresponding Young tableau has two rows of lengths $[p + q, q]$.

And the value of the quadratic Casimir operator $\hat{C}_2(\hat{F}_i) = \sum_i \hat{F}_i^2$ in the representation $D(p, q)$ is:

$$C_2(p, q) = \frac{p^2 + pq + q^2}{3} + p + q \tag{9}$$

For electrons moving on CP^2 geometry under a $U(1)$ magnetic field with flux $S(S \in \mathbb{Z})$ and zero $SU(2)$ field, the $U(2)$ operators in Eq.(A.4,A.5) are corresponding to the right actions of $\hat{F}_1, \hat{F}_2, \hat{F}_3$, and $\hat{F}_8$, which are

$$\begin{aligned}F_i &= 0, \qquad i = 1, 2, 3\\ F_8 &= -\frac{S}{\sqrt{3}},\end{aligned} \tag{10}$$

one can see that representations satisfying Eq. (10) which contain an $SU(2)$ singlet and appropriate value of R_8, require $p - q = S$. Since operators $\hat{R}_{\pm i}$ in Eq. (A.9) are the right action of $\hat{U}_\pm, \hat{V}_\pm$, the Hamiltonian becomes

$$\begin{aligned}H &= \frac{1}{4Mr^2}(\hat{U}_+\hat{U}_- + \hat{U}_-\hat{U}_+ + \hat{V}_+\hat{V}_- + \hat{V}_-\hat{V}_+)\\ &= \frac{1}{2Mr^2}\sum_{i=4}^{7}\hat{F}_i^2 = \frac{1}{2Mr^2}\sum_{i=1}^{8}\hat{F}_i^2 - \hat{F}_8^2\\ &= \frac{1}{2Mr^2}\left[C_2(p, q) - \frac{1}{3}S^2\right].\end{aligned} \tag{11}$$

The energy eigenvalues can then be written by using of Eq. (9) and the relation $p - q = S$:

$$E_q = \frac{1}{2Mr^2}[q(q + 2) + (q + 1)S], \tag{12}$$

the index $q = 0, 1, 2, \ldots$ labels the Landau levels. The $(q + 1)_{th}$ Landau level is $d(p = S + q, q)$-fold degenerate.

For the states on the LLL$(q = 0, p = S)$, the $SU(3)$ representations are $(S, 0)$ which are indeed the symmetric representations with rank-S we

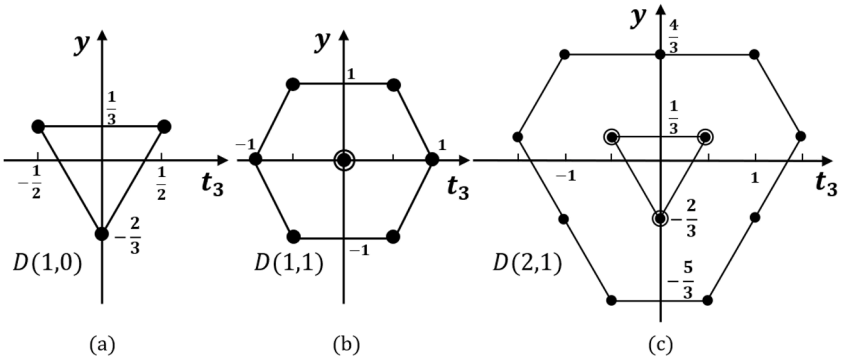

Fig. 3. Some simple multiplets of $SU(3)$.

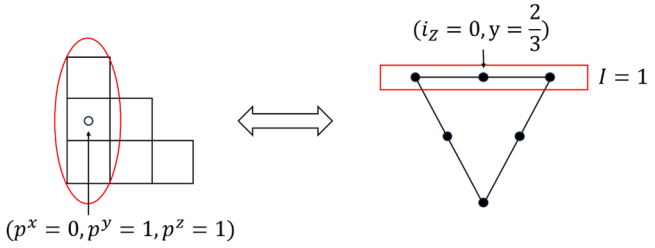

Fig. 4. An example for states in (2,0) representation.

mentioned in the $\mathbb{CP}^k$ case. In this case, the LLL condition Eq. (A.11) becomes

$$\hat{U}_{R-}\Psi = 0, \quad \hat{V}_{R-}\Psi = 0. \tag{13}$$

Using the symmetry of $SU(3)$ representations and the highest weight states $y = \frac{p-q}{3}$, one can immediately see that a state with zero $SU(2)$ charge and nontrivial $U(1)$ charge, $t_3 = 0, y = -\frac{2(p-q)}{3}$, always exists in these $(S,0)$ representations. This state satisfies both Eq. (10) and the LLL condition Eq. (13).

Then we can write down the single particle wavefunctions of the LLL in terms of the local complex $\mathbb{CP}^2$ coordinates according to Eq. (A.13):

$$\psi_{\mathbf{p}} \propto u^{p^x} v^{p^y} w^{p^z}, \tag{14}$$

where (u, v, w) satisfying $|u|^2 + |v|^2 + |w|^2 = 1$, and p^x, p^y, p^z are non-negative integers satisfying $p^x + p^y + p^z = S$. The degeneracy of states on the LLL is given by

$$d(p = S, 0) = \frac{1}{2}(S+1)(S+2). \tag{15}$$

We follow the notation in Ref [33], using a vector $\mathbf{p} = (p^x, p^y, p^z)$ to denote an orbital on the LLL. Since these LLL orbitals form a $SU(3)$ irreducible representation $(S,0)$, the relation between $\mathbf{p}$ and $SU(3)$ quantum numbers isospin(we now use i_z instead of t_3) and hypercharge can be expressed by

$$i_z = \frac{1}{2}(p^y - p^z), \qquad y = \frac{1}{3}S - p^x \tag{16}$$

For the reason that the $(S,0)$ multiplets are nondegenerate in $SU(3)$ weight space, the total $SU(2)$ i_z-spin of each state can also be expressed by $I = \frac{1}{2}(S - p^x)$, with $-I \le i_z \le I$. An example for states in $(2,0)$ representation is shown in Fig. (4).

2.2. Two-body interaction and Haldane pseudopotential

We now consider many-body system by projecting H_I into the LLL. In the second quantized form the two-body interaction Hamiltonian can be written as:

$$H_I = \sum_{\mathbf{p_1},\mathbf{p_2},\mathbf{p_3},\mathbf{p_4}} V_{\mathbf{p_1},\mathbf{p_2},\mathbf{p_3},\mathbf{p_4}} c^\dagger_{\mathbf{p_1}} c^\dagger_{\mathbf{p_2}} c_{\mathbf{p_3}} c_{\mathbf{p_4}} \delta_{\mathbf{p_1}+\mathbf{p_2}=\mathbf{p_3}+\mathbf{p_4}}, \tag{17}$$

where $c^\dagger_{\mathbf{p}}$ and $c_{\mathbf{p}}$ are creation and annihilation operators. The δ function above conserves two quantum numbers(isospin and hypercharge) of $SU(3)$ after scattering.

The matrix elements $V_{\mathbf{p_1},\mathbf{p_2},\mathbf{p_3},\mathbf{p_4}} = \langle \mathbf{p_1}, \mathbf{p_2} | V | \mathbf{p_3}, \mathbf{p_4} \rangle$ can be expanded using the $SU(3)$ generalizations of the Haldane pseudopotential V_l, which amounts to projecting the two-body interaction Hamiltonian onto distinct SU(3) two-particle channels within the $(S,0) \otimes (S,0)$ Hilbert space. By projecting the two-fermion Hilbert space in the $SU(3)$ representation $(S,0) \otimes (S,0)$ onto the channel $(2S - 2l, l)$, the interaction matrix elements $V_{\mathbf{p_1},\mathbf{p_2},\mathbf{p_3},\mathbf{p_4}}$ can be constructed as [34]:

$$V_{\mathbf{p_1},\mathbf{p_2},\mathbf{p_3},\mathbf{p_4}} = \sum_{l,odd}^{m-2} V_l \sum_I C^{(2S-2l,l),I}_{\mathbf{p_1},\mathbf{p_2}} C^{(2S-2l,l),I}_{\mathbf{p_4},\mathbf{p_3}}. \tag{18}$$

Here $C^{(2S-2l,l),I}_{\mathbf{p_1},\mathbf{p_2}}, C^{(2S-2l,l),I}_{\mathbf{p_4},\mathbf{p_3}}$ are the $SU(3)$ Clebsch-Gordan coefficients, with $\mathbf{p}$ labeling a single-particle state in the $(S,0)$ representation. The index l plays a role analogous to the relative angular momentum in the $SU(2)$ Haldane pseudopotential, with smaller l corresponding to shorter-range two-particle correlations. The restriction to odd l follows from the requirement that the two-fermion channel be antisymmetric under particle exchange. m is related to the filling factor $\nu = 1/m$, corresponding to the N-particle Laughlin wavefunction:

$$\Psi_m = \begin{vmatrix} u_1^{p_1^x} v_1^{p_1^y} w_1^{p_1^z} & \dots & u_1^{p_N^x} v_1^{p_N^y} w_1^{p_N^z} \\ \vdots & & \vdots \\ u_N^{p_1^x} v_N^{p_1^y} w_N^{p_1^z} & \dots & u_N^{p_N^x} v_N^{p_N^y} w_N^{p_N^z} \end{vmatrix}^m, \tag{19}$$

where N is the particle number $N = d(S/m, 0)$, while the total number of orbitals is $d(S,0)$. The subscript $i = 1, \dots, N$ labels N particles.

The $SU(3)$ CG coefficient can be constructed following the way in Ref [35]. If the quantum numbers of $\mathbf{p_1}, \mathbf{p_2}$ states in $(S,0)$ representation correspond to (I_1, i_{z1}, y_1) and (I_2, i_{z_2}, y_2) respectively, the state (I, iz, y) in $(2S - 2l, l)$ channel should obey the constraints

$$i_{z1} + i_{z2} = i_z, \quad y_1 + y_2 = y, \quad |I_1 - I_2| \le I \le I_1 + I_2. \tag{20}$$

The same holds for $\mathbf{p_3}, \mathbf{p_4}$ states. These constraints actually preserve the quantum numbers.

In this case, one can find Laughlin wavefunction is actually a unique zero energy ground state of the Hamiltonian Eq. (17), which is in the total $(I_z = 0, Y = 0)$ subspace. The ground state and low-energy excitations spectrum was first derived numerically in Ref [33].

In general, the model we are working with is a fermonic Hamiltonian with $d(S,0) = \frac{1}{2}(S+1)(S+2)$ orbitals and $SU(3)$ invariant interactions. Since the spatial dimension is $d = 4$, the length scale of the system is $[(S+1)(S+2)]^{1/4}$.

3. Ising model on $\mathbb{CP}^2$ space

In this section, we demonstrate the application of the project Hamiltonian method using the example of the Ising transition on the $\mathbb{CP}^2$

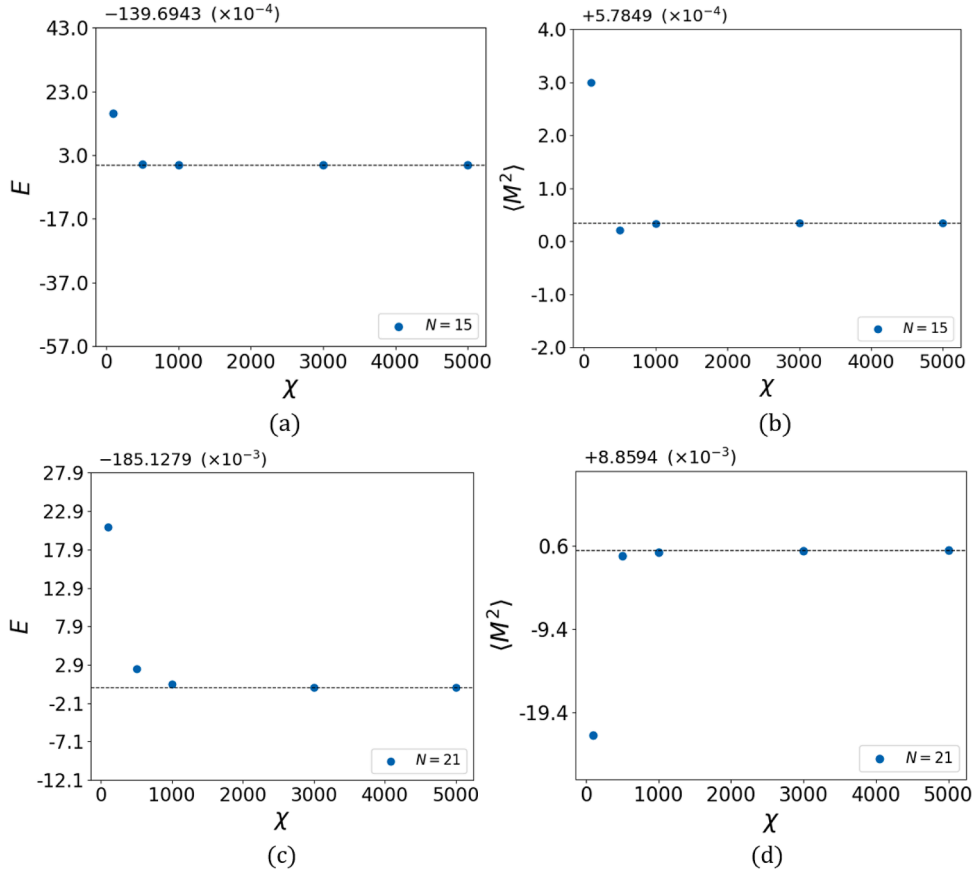

Fig. 5. The convergence of the DMRG results with system size $N = 15$ and $N = 21$, and $V_0 = 1, h = 14.30$. The good convergence is achieved by $\chi > 1000$.

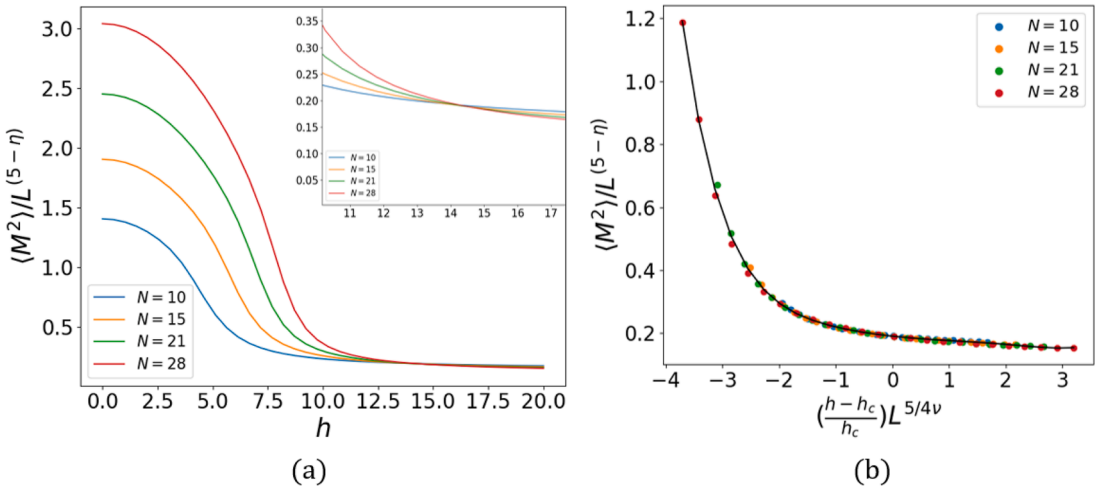

Fig. 6. (a) Finite-size scaling of order parameter $\langle M^2 \rangle / L^{5-\eta}$ with $\eta = 0.0$. $N = \frac{1}{2}(S+1)(S+2)$ is the number of electrons filled in the LLL. The rescaled order parameter crosses at the same point $h_c \approx 14.30$. (b) The data collapse of the rescaled order parameter according to the reduced field strength $(\frac{h-h_c}{h_c})L^{1/\nu}$ with $\nu = 0.5, h_c = 14.30$.

manifold. Our construction is based on the LLL on the $\mathbb{CP}^2$ manifold, as introduced in Section 2. We start with the Ising transition.

In general, the Ising phase transition is described by the effective ϕ^4 theory [36,37]:

$$S = \int d^d x (\nabla\phi)^2 + r\phi^2 + u\phi^4, \tag{21}$$

where ϕ is a real scalar field. Order parameter $\langle\phi\rangle$, relating to the local magnetization, distinguishes symmetry breaking phase ($\langle\phi\rangle \neq 0$) from the symmetric phase ($\langle\phi\rangle = 0$). In the RG analysis, the quartic interaction term is relevant for $d < 4$, so that the theory flows from a free UV fixed point to an interacting IR fixed point [38]. For $d > 4$, the free Gaussian fixed point is stable, where the scaling dimension of the fundamental field ϕ is

$$\Delta_\phi = \frac{d}{2} - 1. \tag{22}$$

Similarly, the scaling dimension of local thermal operator ϵ is $\Delta_\epsilon = d - 2$. Traditionally, in the statistical physics, the critical exponents are

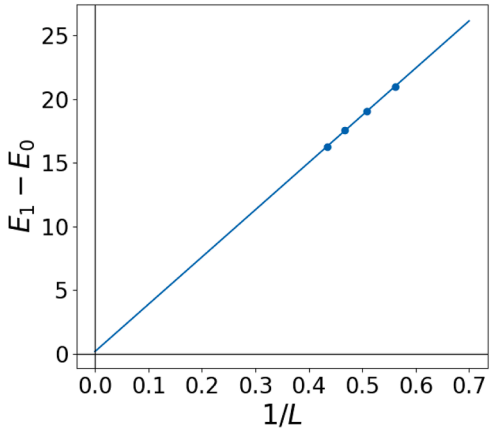

Fig. 7. The finite-size scaling of the lowest excitation gap at the critical point $h_c \approx 14.30$.

widely used to described the critical phenomena. The critical exponents are actually determined by the scaling dimensions of relevant operators as

$$\nu = \frac{1}{d - \Delta_\epsilon}, \tag{23}$$

$$\eta = 2\Delta_\phi - d + 2. \tag{24}$$

For the $\mathbb{CP}^2$ manifold with space-time dimension $d = 5$, we expect $\Delta_\phi = 3/2$ and $\Delta_\epsilon = 3$ exactly, which gives $\eta = 0$ and $\nu = 1/2$ respectively.

3.1. Model and Hamiltonian

Here we consider the quantum Ising model with the Hamiltonian living on $\mathbb{CP}^2$ space, which can be written as

$$H = \int_{\mathbb{CP}^2} d\Omega_a d\Omega_b \, U(\Omega_{ab}) \left[n^0(z_1^a, z_2^a) n^0(z_1^b, z_2^b) - n^z(z_1^a, z_2^a) n^z(z_1^b, z_2^b) \right] - h \int_{\mathbb{CP}^2} d\Omega \, n^x(z_1, z_2). \tag{25}$$

Here z_1, z_2 are the local complex coordinates defined on $\mathbb{CP}^2$ space in Eq. A.12 of Section 2.1, and the subscripts a, b label particles. $n^\alpha(z_1, z_2)$ is the local density operator defined as

$$n^\alpha(z_1, z_2) = [\hat{\psi}_\uparrow^\dagger(z_1, z_2), \hat{\psi}_\downarrow^\dagger(z_1, z_2)] \sigma^\alpha [\hat{\psi}_\uparrow(z_1, z_2), \hat{\psi}_\downarrow(z_1, z_2)]^T \tag{26}$$

with $\sigma^0 = I_{2\times 2}$ and $\sigma^{x,y,z}$ being Pauli matrices and $\hat{\psi}(z_1, z_2)$ is electron annihilation operator. Importantly, the integral on $\mathbb{CP}^2$ manifold is defined by Fubini-Study metric and its Kahler form:

$$\int_{\mathbb{CP}^2} d\Omega = \int_{\mathbb{CP}^2} \frac{1}{(1 + |z_1|^2 + |z_2|^2)^3} d^2 z_1 d^2 z_2. \tag{27}$$

Next we can rewrite the Hamiltonian in the second quantization form since $\hat{\psi}(z_1, z_2) = \sum_{\mathbf{p}} \Psi_{\mathbf{p}} \hat{c}_{\mathbf{p}}$ is the annihilation operator with $\Psi_{\mathbf{p}}$ the single particle wavefunction on $\mathbb{CP}^2$ space (see Eq. (14)) and $\hat{c}_{\mathbf{p}}$ the annihilation operator of Landau orbital, so that we can project the Hamiltonian into the LLL:

$$H = H_{00} + H_{zz} + H_t, \tag{28}$$

$$H_{00} = \sum_{\mathbf{p_1},\mathbf{p_2},\mathbf{p_3},\mathbf{p_4}} V_{\mathbf{p_1},\mathbf{p_2},\mathbf{p_3},\mathbf{p_4}} (\mathbf{c}_{\mathbf{p_1}}^\dagger \mathbf{c}_{\mathbf{p_4}})(\mathbf{c}_{\mathbf{p_2}}^\dagger \mathbf{c}_{\mathbf{p_3}}) \delta_{\mathbf{p_1}+\mathbf{p_2}=\mathbf{p_3}+\mathbf{p_4}}, \tag{29}$$

$$H_{zz} = \sum_{\mathbf{p_1},\mathbf{p_2},\mathbf{p_3},\mathbf{p_4}} V_{\mathbf{p_1},\mathbf{p_2},\mathbf{p_3},\mathbf{p_4}} (\mathbf{c}_{\mathbf{p_1}}^\dagger \sigma^z \mathbf{c}_{\mathbf{p_4}})(\mathbf{c}_{\mathbf{p_2}}^\dagger \sigma^z \mathbf{c}_{\mathbf{p_3}}) \delta_{\mathbf{p_1}+\mathbf{p_2}=\mathbf{p_3}+\mathbf{p_4}}, \tag{30}$$

$$H_t = -h \sum_{\mathbf{p}} \mathbf{c}_{\mathbf{p}}^\dagger \sigma^x \mathbf{c}_{\mathbf{p}}, \tag{31}$$

where $\mathbf{c}_{\mathbf{p}}^\dagger = (c_{\mathbf{p}\uparrow}^\dagger, c_{\mathbf{p}\downarrow}^\dagger)$ creates spinful electrons on the $\mathbf{p}$ Landau orbital as defined in the section Section 2.2. The interaction parameter $V_{\mathbf{p_1},\mathbf{p_2},\mathbf{p_3},\mathbf{p_4}}$ is related to the $SU(3)$ Haldane pseudopotential V_l as before but now connected to the interlayer interaction in a spinful system:

$$V_{\mathbf{p_1},\mathbf{p_2},\mathbf{p_3},\mathbf{p_4}} = \sum_l V_l \sum_I C_{\mathbf{p_1},\mathbf{p_2}}^{(2S-2l,l),I} C_{\mathbf{p_4},\mathbf{p_3}}^{(2S-2l,l),I}. \tag{32}$$

The first two terms of the Hamiltonian, $H_{00} + H_{zz}$ correspond to short-ranged density-density interactions in real space, which yields the Ising ferromagnet as the ground state. The term H_t is the transverse field, which produces paramagnet as the ground state. The competing of these two terms leads to a phase transition from Ising ferromagnet to the paramagnet, and a Ising-type transition in between. We will verify this expectation later.

In practice, we consider the LLL is filled by $N = \frac{1}{2}(S+1)(S+2)$ electrons in total to process the phase transition of Ising model (The degeneracy of the LLL please see Eq. (15)). The Hamiltonian of this model has Ising $\mathbb{Z}_2$ symmetry: $\mathbf{c}_{\mathbf{p}} \to \sigma^x \mathbf{c}_{\mathbf{p}}$, $SU(3)$ symmetry since all orbitals $\mathbf{p}$ in the LLL are in the $(S, 0)$ representation of $SU(3)$, and particle-hole symmetry: $\mathbf{c}_{\mathbf{p}} \to i\sigma^y \mathbf{c}_{\mathbf{p}}{}^*, i \to -i$.

In this paper, the Haldane pseudopotential involves channels with $l = 0, 1$. When $h = 0$ and $V_0, V_1 > 0$, the $\mathbb{Z}_2$ symmetry breaks spontaneously, resulting in 2-fold degenerate Ising ferromagnetism ground states where the many-body state is either fully spin-up or fully spin-down. When $h \gg V_0, V_1$, the ground state is a paramagnetic phase preserves Ising symmetry. In this work, we set $V_1 = 1$ as energy unit and vary V_0 and h to study the phase transition.

3.2. Numerical method

In this paper, we solve the Hamiltonian H numerically on finite systems. Since the number of the LLL orbitals increases fast by varying the monopole charge S (see Eq. 15), the model is solved numerically by using exact diagonalization (ED) for smaller size ($N \leq 15$) and density matrix renormalization group (DMRG) for larger size ($N > 15$).The ED calculations are performed using our own code, while the DMRG simulations are implemented with the ITensor library [39].

Notice that the Hilbert space dimension of this half-filled spinful system grows exponentially, resulting in an extremely high computational cost. However, the $SU(3)$ symmetry enables a substantial reduction of the Hilbert space dimension. As discussed in Section 2.2, the total isospin and hypercharge of electrons are conserved under scattering processes, providing two good quantum numbers (defined as Eq. (16)) by which the Hilbert space can be block-diagonalized. For instance, the block with the total quantum numbers $(I_z, Y) = (0, 0)$ is typically chosen, since it contains the ground state as well as the majority of low-lying excitations. Within this symmetry sector, the Hilbert space dimension is significantly reduced approximately as $90, 6028, 2.24 \times 10^6, 4 \times 10^9$ compared to the full space, according to $N = 6, 10, 15, 21$, respectively. In this way, the ED method can be applied to the systems with $N \leq 15$ in the present model. For the ED calculations, we have benchmarked the case with $N_o = 28, N_e = 6$ in the 1/3-filled quantum Hall system studied in Ref [33].

For the cases with $N = 21, 28$, the Hilbert space becomes too large for ED. Therefore, the DMRG method is employed to obtain the ground state and low-lying excitations. A small difference from the previous works is, in the current case, the Landau orbitals donot form a simple 1d structure, instead they form a triangular-like structure (see Fig. 4) as an example. We can assign each Landau orbital with a matrix to represent the variational space and we find the usual optimization process still works. In the DMRG calculations, the maximum bond dimension χ and the truncation error ϵ are carefully adjusted to balance computational cost and accuracy. In this work, we set the maximum bond dimension up to $\chi = 5000$ and a truncation error below $\epsilon = 10^{-8}$. The convergence of the results is further checked by increasing χ and verifying the stability of the energy and order parameters as shown in Fig. (5).

3.3. Numerical results

In this model, the $\mathbb{Z}_2$ order parameter of the transition is:

$$M = \frac{1}{2}\sum_{\mathbf{p}} \mathbf{c}_{\mathbf{p}}^{\dagger}\sigma^{z}\mathbf{c}_{\mathbf{p}}. \tag{33}$$

The phase transition is then obtained by the finite size scaling of the order parameter M. In this paper, we employ the curve-crossing method and the data-collapse approach to study the phase transition, taking into account different system sizes.

Fig. (6a) illustrates the rescaled order parameter $\langle M^2\rangle/L^5$ as a function of the transverse field strength h for various system sizes N with $V_0 = 10$. The curves cross at h_c which signals the phase transition point. For $h < h_c$, the finite-size order parameter grows with system sizes, confirming the ferromagnetic phase. For $h > h_c$ the order parameter reduces with the system sizes, indicating the disordered phase. These results confirm a phase transition from ordered Ising ferromagnetism to disordered paramagnetic phase.

Around the phase transition point, the order parameter should satisfy some finite-size scaling behavior. In specific, the magnetic order should obey

$$\langle M^2\rangle/L^{5-\eta} = f((\frac{h-h_c}{h_c})L^{1/\nu}) \tag{34}$$

where the critical exponent η, ν can be estimated from the field theory analysis in Section 3 and h_c is the critical field. Fig. (6b) depicts the data collapse for according to Eq. (34), where a polynimial function is also used to fit our data. The best fit gives the critical field $h_c \approx 14.30$.

In addition, the transition point can be identified by calculating the lowest spin excitation gap. Since flipping a spin orientation costs finite energy in the paramagnet phase, the spin excitation gap should be nonzero. However, at the critical point, the system becomes gapless. Fig. (7) shows the lowest excitation gaps with respect to field strength and the finite-size scaling of the lowest excitation gap at the critical point. The transition point is determined to be $h_c \approx 14.30$.

Since the Ising model can be described by the field theory of a scalar field ϕ with a ϕ^4 coupling which is irrelevant for $d > 4$, our $(4+1)$-D Ising model is in the case that the mean field theory works. The theoretical predictions for the critical exponents in this case are $\nu = 0.5, \eta = 0$ and the scaling dimension of the order parameter is $\Delta_\phi = \frac{D-2+\eta}{2} = 1.5$, which nicely fit our numerical results.

4. Summary and discussion

To summarize, we first reviewed the single particle states on $2k$ dimensional manifold CP^k and focused on CP^2 space with $U(1)$ background magnetic field in details by using the $SU(3)$ Lie algebra. We constructed a many-body system to numerically study a four-dimensional quantum Ising phase transition. Under strong magnetic field h_x, the ground state state is paramagnetic, while under small magnetic field the ground state is ferromagnetic with all the spins having the same orientation. The phase transition point is numerically determined by the ordinary order parameter. The obtained critical exponents meet the prediction of Landau-Ginzburg theory and conformal analysis. To our best knowledge, this is the first attempt of the quantum phase transition in $(4+1)$ spacetime dimension. We believe this work opens a way for the study of phase transitions in higher space-time dimensional geometry. We envision that our approach can be generalized to $\mathbb{CP}^k$ manifold or other higher-dimensional space such as S^4, which has been illustrated that $\mathbb{CP}^3$ with a $U(1)$ field is equivalent to an $SU(2)$ instanton on S^4 [25]. Furthermore, one may also take into account the $SU(k)$ gauge field. Besides, this approach can also be applied to other universalities such as the XY model. The corresponding conformal field theory are left for future research.

CRediT authorship contribution statement

Xue Meng: Writing – review & editing, Writing – original draft, Software, Methodology, Investigation, Funding acquisition, Formal analysis, Data curation, Conceptualization; **Junwen Zhao:** Writing – review & editing; **Wei Zhu :** Writing – review & editing, Supervision, Project administration, Conceptualization; **Congjun Wu:** Supervision.

Data availability

Data will be made available on request.

Declaration of competing interest

The authors declare that they have no known competing financial interests or personal relationships that could have appeared to influence the work reported in this paper.

Acknowledgments

W.Z. thanks J. Wang for introducing $\mathbb{CP}^2$ geometry to us. W.Z. thanks Yin Tang for insightful discussion. This work was supported by National Science Foundation of China under project number 12474144.

Appendix A. Group theoretic analysis on $\mathbb{CP}^k$

In this appendix, we present a general discussion of Landau-level quantization and related constructions on the complex projective space $\mathbb{CP}^k$, which are $2k$-dimensional Kähler manifolds and can be viewed as coset space

$$\mathbb{CP}^k = \frac{SU(k+1)}{U(k)} \sim \frac{SU(k+1)}{SU(k)\times U(1)}, \tag{A.1}$$

which defines natural background $U(1)$ and $SU(k)$ magnetic fields. The wavefunctions can be obtained as functions on $SU(k+1)$ with specific transformation properties under $U(k)$, which can be given by the Wigner D-functions. In group theory, for an group element $g \in SU(k+1)$, we can define left and right $SU(3)$ actions by

$$\hat{L}_a g = T_a g, \qquad \hat{R}_a g = g T_a, \tag{A.2}$$

where T_a are the $SU(k+1)$ generators. The right operators $\hat{R}_a$ corresponding to covariant derivatives consist of raising and lowering operators from one Landau level to the next, while the left operators $\hat{L}_a$ correspond to magnetic translations which rotate the eigenstates on the manifold preserving the Landau level index. This formalism is similar to the well-known case on sphere ($\mathbb{CP}^1$) one may be familiar with [40].

As T_a form a basis of Lie algebra of $SU(k+1)$ in the fundamental representation, they are chosen to obey

$$[T_a, T_b] = i f_{abc} T_c, \qquad \mathrm{Tr}(T_a T_b) = \frac{1}{2}\delta_{ab}, \tag{A.3}$$

where f_{abc} are the structure constants of $SU(k+1)$.

Since the dimensions of Lie groups $SU(k+1)$ and their subgroups $U(k) \sim SU(k)\times U(1)$ are k^2+2k and k^2, respectively, we can denote the $SU(k)$ and $U(1)$ in $U(k) \subset SU(k+1)$: $R_\alpha, \alpha = 1, 2, \ldots, k^2-1$ will denote $SU(k)$ generators and R_{k^2+2k} will denote the generator in the $U(1)$ direction.

In this paper we always focus only on the $U(1)$ Abelian background and in the absence of $SU(k)$ non-Abelian background charge. Therefore, with the background field along the $U(1)$ direction, the wavefunctions for the Landau level on $\mathbb{CP}^k$ are singlets under the subgroup $SU(k)_R$ and carry nontrivial $U(1)_R$ charge. So that the quantum numbers for R_a are constrained to be

$$R_\alpha = 0, \qquad \alpha = 1, 2, \ldots, k^2-1 \tag{A.4}$$

$$R_{k^2+2k} = -S\frac{k}{\sqrt{2k(k+1)}}, \tag{A.5}$$

where S is the $U(1)$ magnetic charge with a form of Br^2 with B the magnetic field and r the radius of the $\mathbb{CP}^k$, respectively. Similar to Dirac-type quantization conditions, S is an non-negative integer. The reason that the $U(1)$ charge takes the form in Eq. (A.5) will be discussed later.

There are $2k$ generators of $SU(k+1)$ which are not in $U(k)$. Thus we denote these $SU(k+1)$ generators which are in the complement of $U(k)$ as $R_\beta, \beta = 1, 2, \dots, 2k$. These can be further separated into the k raising type R_{+i} and k lowering type R_{-i} with the definition $R_{\pm i} = R_{2i-1} \pm iR_{2i}, i = 1, 2, \dots, k$. The covariant derivatives on $\mathbb{CP}^k$ are then given by

$$D_{\pm i} = i\frac{\hat{R}_{\pm i}}{r}. \tag{A.6}$$

By using the structure constants and Eq. (A.5), the commutator between R_+ and R_- is

$$\begin{aligned}[\hat{R}_{+i}, \hat{R}_{-j}] &= if_{ij\alpha}\hat{R}_\alpha + \delta_{ij}\sqrt{\frac{2(k+1)}{k}}\hat{R}_{k^2+2k} \\ &= -S\delta_{ij},\end{aligned} \tag{A.7}$$

with $\hat{R}_a$ a generator of $SU(k)$ and zero $SU(k)$ background charge condition. With this relation, the commutator of $D_\pm$ in Eq. (A.6) becomes $[D_{+i}, D_{-i}] \sim B$. Thus, the form of $U(1)$ charge defined in Eq. (A.5) is consistent with the fact that the commutator of covariant derivatives is the magnetic field.

The Laplacian for $\mathbb{CP}^k$ space is related to covariant derivatives, given by $-\nabla^2 = \frac{1}{2}(D_{+i}D_{-i} + D_{-i}D_{+i})$. Thus, the Hamiltonian for the QHE problem is proportional to this covariant Laplacian:

$$H\Psi = -\frac{1}{4M}\sum_i (D_{+i}D_{-i} + D_{-i}D_{+i})\Psi, \tag{A.8}$$

where M is the electron's mass. With zero $SU(k)$ background field Eq. (A.4), the Hamiltonian can be written as

$$\begin{aligned}H\Psi &= \frac{1}{4Mr^2}\sum_i (\hat{R}_{+i}\hat{R}_{-i} + \hat{R}_{-i}\hat{R}_{+i})\Psi \\ &= \frac{1}{2Mr^2}\Big(\sum_a^{k^2+2k} R_a^2 - R_{k^2+2k}^2\Big)\Psi.\end{aligned} \tag{A.9}$$

Therefore, the corresponding energy eigenvalues are:

$$\begin{aligned}E &= \frac{1}{2Mr^2}(C_2^{SU(k+1)} - R_{k^2+2k}^2) \\ &= \frac{1}{2Mr^2}(C_2^{SU(k+1)} - \frac{k}{2(k+1)}S^2),\end{aligned} \tag{A.10}$$

where C_2 is the eigenvalue of the quadratic Casimir operator of the $SU(k+1)$ group.

One can use the commutator in Eq. (A.7) and see that H is an increasing function which is proportional to $\sum_i \hat{R}_{+i}\hat{R}_{-i}$, apart from some additive constants. Hence the lowest Landau level should satisfy the condition

$$\hat{R}_{-i}\Psi = 0. \tag{A.11}$$

The conditions Eq. (A.4),(A.5),(A.11) completely fix the representation of LLL, which imply the symmetric rank S representation of $SU(k+1)$ that contains the lowest weight state with nontrivial $U(1)$ charge and $SU(k)$ singlet.

Recalling that $\mathbb{CP}^k$ is a $2k$-dimensional complex projective space and can be parameterized by $k+1$ complex coordinates $u_\alpha, \alpha = 0, 1, 2, \dots, k$, such that $\bar{u}^\alpha u_\alpha = 1$ with the identification $u_\alpha \sim e^{i\theta}u_\alpha$. Further, we can introduce local complex coordinates $z_i = x_i + iy_i$ by writing

$$u = \frac{1}{\sqrt{1+\bar{z}\cdot z}}\begin{pmatrix}1\\ z_1\\ \vdots\\ z_k\end{pmatrix} \tag{A.12}$$

In terms of u, the basis for functions on $\mathbb{CP}^k$ can be given by $\{\phi_l\} : \phi_l = \bar{u}^{\alpha_1}\dots\bar{u}^{\alpha_l}u_{\beta_1}\dots u_{\beta_l}$, with l an integer value. For a fixed value of l, this form is symmetric for all the upper indices for $\bar{u}$ or for all the lower indices for u. Since the representations of $SU(k+1)$ for the LLL are totally symmetric and of rank S as mentioned before, the wavefunctions are then derived in local coordinates as

$$\begin{aligned}\Psi_{p_0p_1\dots p_k} &= \left[\frac{S!}{p_0!p_1!\dots p_k!}\right]^{\frac{1}{2}}\frac{z_0^{p_0}z_1^{p_1}\dots z_k^{p_k}}{(1+\bar{z}\cdot z)^{S/2}} \\ &\sim u_0^{p_0}u_1^{p_1}\dots u_k^{p_k},\end{aligned} \tag{A.13}$$

with

$$S = p_0 + p_1 + \dots + p_k. \tag{A.14}$$

Here $0 \le p_i \le S$. The condition Eq. (A.11) is then a holomorphicity condition that implies the wavefunctions are holomorphic of z.

The degeneracy of states in the LLL is then given by the dimension of this symmetric S-rank $SU(k+1)$ representation as

$$N = \frac{(k+S)!}{k!S!}. \tag{A.15}$$

References

[1] R.G. Leigh, M.J. Strassler, Exactly marginal operators and duality in four dimensional n = 1 supersymmetric gauge theory, Nucl. Phys. B 447 (1) (1995) 95-133. https://doi.org/10.1016/0550-3213(95)00261-p

[2] N. Seiberg, Five dimensional SUSY field theories, non-trivial fixed points and string dynamics, Phys. Lett. B 388 (4) (1996) 753-760. https://doi.org/10.1016/s0370-2693(96)01215-4

[3] A. Hebecker, 5D super-Yang-mills theory in 4d superspace, superfield brane operators, and applications to orbifold GUTs, Nucl. Phys. B 632 (1-3) (2002) 101-113. https://doi.org/10.1016/s0550-3213(02)00253-5

[4] W. Zhu, C. Han, E. Huffman, J.S. Hofmann, Y.-C. He, Uncovering conformal symmetry in the 3D ising transition: state-Operator correspondence from a quantum fuzzy sphere regularization, Phys. Rev. X 13 (2023) 021009. https://doi.org/10.1103/PhysRevX.13.021009

[5] A.M. Läuchli, L. Herviou, P.H. Wilhelm, S. Rychkov, Exact Diagonalization, Matrix Product States and Conformal Perturbation Theory Study of a 3D Ising Fuzzy Sphere Model, 2025, 2504.00842 https://arxiv.org/abs/2504.00842.

[6] C. Han, L. Hu, W. Zhu, Conformal operator content of the wilson-Fisher transition on fuzzy sphere bilayers, Phys. Rev. B 110 (2024) 115113. https://doi.org/10.1103/PhysRevB.110.115113

[7] A. Dey, L. Herviou, C. Mudry, A.M. Läuchli, Conformal Data for the O(3) Wilson-Fisher CFT from Fuzzy Sphere Realization of Quantum Rotor Model, 2025, 2510.09755 https://arxiv.org/abs/2510.09755.

[8] R. Fan, J. Dong, A. Vishwanath, Simulating the non-unitary Yang-Lee conformal field theory on the fuzzy sphere, 2025, 2505.06342 https://arxiv.org/abs/2505.06342.

[9] E.A. Cruz, I.R. Klebanov, G. Tarnopolsky, Y. Xin, Yang-Lee Quantum Criticality in Various Dimensions, 2025, 2505.06369 https://arxiv.org/abs/2505.06369.

[10] J.E. Miro, O. Delouche, Flowing from the Ising Model on the Fuzzy Sphere to the 3D Lee-Yang CFT, 2025, 2505.07655 https://arxiv.org/abs/2505.07655.

[11] S. Yang, Y.-G. Yue, Y. Tang, C. Han, W. Zhu, Y. Chen, Microscopic study of the three-dimensional potts phase transition via fuzzy sphere regularization, Phys. Rev. B 112 (2025) 024436. https://doi.org/10.1103/x1qn-x6xb

[12] Y.-C. He, Free real scalar CFT on fuzzy sphere: spectrum, algebra and wavefunction ansatz, 2025, 2506.14904 https://arxiv.org/abs/2506.14904.

[13] J. Taylor, C. Voinea, Z. Papićxst, R. Fan, Conformal scalar field theory from Ising tricriticality on the fuzzy sphere, 2025, https://arxiv.org/abs/2506.22539. 2506.22539

[14] Z. Zhou, L. Hu, W. Zhu, Y.-C. He, SO(5) Deconfined phase transition under the fuzzy-Sphere microscope: approximate conformal symmetry, pseudo-Criticality, and operator spectrum, Phys. Rev. X 14 (2024) 021044. https://doi.org/10.1103/PhysRevX.14.021044

[15] B.-B. Chen, X. Zhang, Y. Wang, K. Sun, Z.Y. Meng, Phases of (2 + 1)D SO(5) nonlinear sigma model with a topological term on a sphere: multicritical point and disorder phase, Phys. Rev. Lett. 132 (2024) 246503. https://doi.org/10.1103/PhysRevLett.132.246503

[16] B.-B. Chen, X. Zhang, Z.Y. Meng, Emergent conformal symmetry at the multicritical point of (2 + 1)D SO(5) model with wess-Zumino-Witten term on a sphere, Phys. Rev. B 110 (2024) 125153. https://doi.org/10.1103/PhysRevB.110.125153

[17] M. Ippoliti, R.S.K. Mong, F.F. Assaad, M.P. Zaletel, Half-filled landau levels: a continuum and sign-free regularization for three-dimensional quantum critical points, Phys. Rev. B 98 (2018) 235108. https://doi.org/10.1103/PhysRevB.98.235108

[18] C. Voinea, R. Fan, N. Regnault, Z. Papić, Regularizing 3D conformal field theories via anyons on the fuzzy sphere, Phys. Rev. X 15 (2025) 031007. https://doi.org/10.1103/bf4k-phl9

[19] L. Hu, Y.-C. He, W. Zhu, Solving conformal defects in 3D conformal field theory using fuzzy sphere regularization, Nat. Commun. 15 (1) (2024) 3659. https://doi.org/10.1038/s41467-024-47978-y

[20] Z. Zhou, D. Gaiotto, Y.-C. He, Y. Zou, The g-function and defect changing operators from wavefunction overlap on a fuzzy sphere, SciPost Phys. 17 (2024) 021. https://doi.org/10.21468/SciPostPhys.17.1.021

[21] Z. Zhou, Y. Zou, Studying the 3d ising surface CFTs on the fuzzy sphere, SciPost Phys. 18 (2025) 031. https://doi.org/10.21468/SciPostPhys.18.1.031
[22] M. Dedushenko, Ising BCFT from Fuzzy Hemisphere, 2024, 2407.15948
[23] F.D.M. Haldane, Fractional quantization of the hall effect: a hierarchy of incompressible quantum fluid states, Phys. Rev. Lett. 51 (1983) 605–608. https://doi.org/10.1103/PhysRevLett.51.605
[24] S.-C. Zhang, J. Hu, A four-Dimensional generalization of the quantum hall effect, Science 294 (5543) (2001) 823–828. https://doi.org/10.1126/science.294.5543.823
[25] D. Karabali, V. Nair, Quantum hall effect in higher dimensions, Nucl. Phys. B 641 (2002) 533–546. https://doi.org/10.1016/S0550-3213(02)00634-X
[26] D. Karabali, Aspects of higher dimensional quantum hall effect: bosonization, entanglement entropy, PoS CORFU2021 (2022) 237. 2203.14350https://doi.org/10.22323/1.406.0237
[27] T.T. Wu, C.N. Yang, Dirac monopole without strings: monopole harmonics, Nucl. Phys. B 107 (3) (1976) 365–380. https://doi.org/10.1016/0550-3213(76)90143-7
[28] T.T. Wu, C.N. Yang, Some properties of monopole harmonics, Phys. Rev. D 16 (1977) 1018–1021. https://doi.org/10.1103/PhysRevD.16.1018
[29] D. KARABALI, V.P. NAIR, S. RANDJBAR-DAEMI, FUZZY SPACES, THE M(ATRIX) MODEL AND THE QUANTUM HALL EFFECT, pp. 831–875. https://doi.org/10.1142/9789812775344_0021
[30] D. Karabali, V.P. Nair, Quantum hall effect in higher dimensions, matrix models and fuzzy geometry, J. Phys. A: Math. Gen. 39 (41) (2006) 12735. https://doi.org/10.1088/0305-4470/39/41/S05
[31] D. Karabali, V.P. Nair, Geometry of the quantum hall effect: an effective action for all dimensions, Phys. Rev. D 94 (2016) 024022. https://doi.org/10.1103/PhysRevD.94.024022
[32] W. Greiner, B. Müller, Quantum Mechanics: Symmetries, Springer-Verlag Berlin Heidelberg, 2 edition, 1994. Original German published by Verlag Harri Deutsch, Thun, 1984, 1992. https://doi.org/10.1007/978-3-642-57976-9
[33] J. Wang, S. Klevtsov, M.R. Douglas, Fractional quantum hall states on $\mathbb{CP}^2$ space, Phys. Rev. Res. 5 (2023) 023042. https://doi.org/10.1103/PhysRevResearch.5.023042
[34] C.-H. Chern, D.-H. Lee, New family of models for incompressible quantum liquids in $d \geq 2$, Phys. Rev. Lett. 98 (2007) 066804. https://doi.org/10.1103/PhysRevLett.98.066804
[35] A.C.N. Martins, M.W. Suffak, H. de Guise, SU(3) Clebsch-Gordan coefficients and some of their symmetries, 2019, 1909.09055
[36] S. Sachdev, Quantum Phase Transitions, Cambridge University Press, 2 edition, 2011. https://doi.org/10.1017/CBO9780511973765
[37] C. Domb, Phase transitions and critical phenomena, Elsevier, 2000.
[38] K.G. Wilson, M.E. Fisher, Critical exponents in 3.99 dimensions, Phys. Rev. Lett. 28 (1972) 240–243. https://doi.org/10.1103/PhysRevLett.28.240
[39] M. Fishman, S.R. White, E.M. Stoudenmire, The ITensor software library for tensor network calculations, SciPost Phys. Codebases (2022) 4. https://doi.org/10.21468/SciPostPhysCodeb.4
[40] M. Greiter, Landau level quantization on the sphere, Phys. Rev. B 83 (2011) 115129. https://doi.org/10.1103/PhysRevB.83.115129